

This is the accepted manuscript made available via CHORUS. The article has been published as:

# Finite Temperature Green's Function Approach for Excited State and Thermodynamic Properties of Cool to Warm Dense Matter

J.J. Kas and J.J. Rehr

Phys. Rev. Lett. **119**, 176403 — Published 25 October 2017

DOI: [10.1103/PhysRevLett.119.176403](https://doi.org/10.1103/PhysRevLett.119.176403)

# Finite temperature Green’s function approach for excited state and thermodynamic properties of cool to warm dense matter

J. J. Kas and J. J. Rehr

*Dept. of Physics, Univ. of Washington Seattle, WA 98195*

(Dated: September 21, 2017)

We present a finite-temperature extension of the retarded cumulant Green’s function for calculations of excited-state, correlation, and thermodynamic properties of electronic systems. The method incorporates a cumulant to leading order in the screened Coulomb interaction  $W$ , and improves on the  $GW$  approximation of many-body perturbation theory. Results for the homogeneous electron gas are presented for a wide range of densities and temperatures, from cool to warm dense matter regimes, which reveal several hitherto unexpected properties. For example, correlation effects remain strong at high  $T$  while the exchange-correlation energy becomes small; also the spectral function broadens and damping increases with temperature, blurring the usual quasi-particle picture. These effects are evident e.g., in Compton scattering which exhibits many-body corrections that persist at normal densities and intermediate  $T$ . The approach also yields exchange-correlation energies and potentials in good agreement with existing methods.

PACS numbers: 71.15.-m, 31.10.+z, 71.10.-w

Keywords: Green’s function, cumulant,  $GW$ , DFT, Excited States

Finite temperature (FT) effects in electronic systems are both of fundamental interest and practical importance. These effects vary markedly depend on whether the temperature  $T$  is larger or smaller than the Fermi temperature  $T_F$  (typically a few eV). At “cool” temperatures ( $T \ll T_F$ ), electrons are nearly degenerate, and Fermi factors and excitations such as phonons dominate the thermal behavior [1–3]. In contrast, thermal occupations become nearly semi-classical and plasmon excitations are important in the warm-dense-matter (WDM) regime ( $T \approx T_F$ ) where condensed matter is partially ionized. Recently there has been considerable interest in both experimental and theoretical investigations of WDM ranging from laser-shocked systems and inertial confinement fusion to astrophysics [4–6]. Many such studies focus on thermodynamic properties using FT generalizations of density functional theory (DFT) [7–10]. Although in principle, DFT is exact [11–13], practical applications are based on approximate exchange-correlation functionals [9, 14, 15] fit to the electron gas [16–21]. However, these approaches have various limitations. First, many materials properties such as band-gaps, optical spectra, photoemission, and Compton scattering depend on quasi-particle effects and inelastic losses [22, 23], which require extensions of DFT and TDDFT [24–26] for accurate treatments. Although methods like quantum Monte-Carlo (QMC) can provide accurate correlation energies [16, 17, 21], they are not directly applicable to excited state and spectral properties. Second, fits to exchange-correlation functionals can exhibit unphysical behavior outside the range of theoretical data [14]. Third, while Green’s function (GF) methods within many-body perturbation theory (MBPT) provide a systematic framework for excited state and thermodynamic equilibrium properties [27], and are widely used at low  $T$  [1–3, 28] and even nuclear matter [29], relatively little

attention has been devoted to their use in WDM [30, 31].

In an effort to address these limitations, we have developed an (FT) extension of the retarded cumulant Green’s function [32, 33] for calculations of excited state, correlation, and thermodynamic properties. Notably the approach permits a physical interpretation of correlation effects in terms of the cumulant, which is directly related to the electron self-energy. The cumulant approach improves on the  $GW$  approximation of MBPT for spectral properties [34], and is exact for certain models [35]. For example, in contrast to  $GW$ , the cumulant approach explains the multiple-plasmon satellites observed in x-ray photoemission spectra (XPS) [34, 36–39]. At  $T = 0$  the method has been applied in a variety of contexts [38, 40–43]. As an application relevant to FT DFT, we have implemented the approach for the homogeneous electron gas (HEG) over a broad range of densities and temperatures. Our results show that besides reductions in quasi-particle energy shifts (e.g., band-gaps) with increasing  $T$ , the spectral function broadens and excited states become strongly damped, corresponding to short mean-free-paths and smeared-out band-structure, blurring the conventional quasi-particle picture. Finally thermodynamic properties and exchange-correlation internal energies are calculated using the Galitskii-Migdal-Koltun (GMK) sum rule [27, 44, 45], which serve as a check on our approximations and yield results that compare well with accurate PIMC (path-integral Monte-Carlo) calculations [16].

Briefly our approach is based on the retarded Green’s function formalism [1, 27], using a FT extension of the cumulant approximation [32, 46]. Below we outline the key elements of the approach; additional technical details of the formalism and our implementation are given in Supplementary Material. The retarded one-particle Green’s function  $G(\omega)$  satisfies a Dyson equation  $G = G^0 + G^0 \Sigma G$

[47], where  $\Sigma$  is the FT retarded self-energy. Formally  $\Sigma$  can be obtained by analytical continuation of the Matsubara self-energy to real energies, and can be expressed in terms of  $G$ , the screened Coulomb interaction  $W = \epsilon^{-1}v$ , and a vertex function  $\Gamma$  [32, 47]. Here and below matrix indices and arguments are suppressed, and we use atomic units  $e = \hbar = m = 1$  unless otherwise specified. Most practical calculations ignore vertex corrections ( $\Gamma = 1$ ). With this restriction, a variety of approximations are used: The widely used  $GW$  approximation is based on the Dyson equation and MBPT to first order in  $W$ ; then  $\Gamma = 1$  and  $G = G^0 + G^0 \Sigma^{GW} G$  [32, 48]. As an approximation the FT quasi-particle self-consistent  $GW$  approach (QPSCGW) [30] starts with the GF on the Keldysh contour; while self-consistency is included, vertex corrections, satellites, and damping are ignored.

The retarded cumulant approach focused on here work is based on an exponential representation of  $G$  in the time-domain for a given single-particle state  $k$ , in which  $G$  is assumed to be diagonal, and the spectral function  $A_k(\omega)$  is obtained from its Fourier transform,

$$G_k(t) = -i\theta(t)e^{-i\varepsilon_k^x t} \tilde{C}_k(t), \quad (1)$$

$$A_k(\omega) = -\frac{1}{\pi} \text{Im} \int d\omega e^{i\omega t} G_k(t). \quad (2)$$

This formulation builds in implicit dynamic vertex corrections [32, 36], and can be justified using the quasi-boson approximation [32], in which electron-electron interactions are represented in terms of electrons coupled to bosonic excitations. An advantage is that exchange and correlation contributions are separable  $C_k(t) = -i\Sigma_k^x t + \tilde{C}_k(t)$ , and all correlation effects are included in the dynamic part  $\tilde{C}_k(t)$ . Here  $\Sigma_k^x = \Sigma_{\mathbf{q}} n_{\mathbf{k}-\mathbf{q}} v_{\mathbf{q}}$  is the exchange part of the FT Hartree-Fock one-particle energy,  $\varepsilon_k^x = \varepsilon_k + \Sigma_k^x$ ,  $\varepsilon_k = k^2/2$  the bare energy,  $v_{\mathbf{q}} = 4\pi/q^2$  the bare Coulomb interaction, and  $n_{\mathbf{k}}$  are single-particle occupation numbers. More elaborate GF methods exist at least in principle, including higher order MBPT [49, 50], and dynamical mean-field theory with impurity Green's function's [51, 52], but are more demanding computationally.

The FT cumulant formulation is directly analogous to that for  $T = 0$  [33], apart from implicit temperature dependence in its ingredients. The form of the retarded cumulant  $C_k(t)$  can be obtained by matching terms in powers of  $W$  to those of the Dyson equation [33, 34]. Carried to all orders the cumulant GF is formally exact; however, by limiting the theory to first order in  $W$ ,  $G^0 C = G^0 \Sigma^{GW} G^0$ , the retarded GW self energy  $\Sigma^{GW}$  is sufficient to define the FT cumulant.  $\tilde{C}(t)$  has a Landau representation, which implies a positive-definite spectral

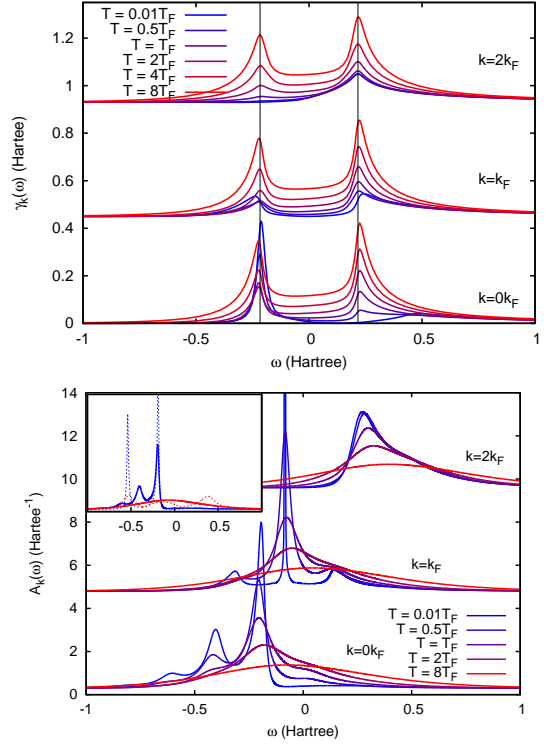


FIG. 1: (Color online) FT retarded cumulant kernel  $\gamma_k(T, \omega)$  (top); and spectral function  $A_k(T, \omega)$  for the HEG (bottom) for  $r_s = 4$ . Vertical lines in the top plot are shown at  $\pm\omega_p$ . Note the enhanced symmetry of both  $\gamma_k$  and  $A_k$  at high- $T$ . The inset shows a comparison of the cumulant (solid) and GW (dashes) spectral functions at  $k = 0$  for the lowest and highest temperatures.

function and conserves spectral weight [32, 35, 53],

$$\tilde{C}_k(t) = \int d\omega \frac{\gamma_k(\omega)}{\omega^2} (e^{-i\omega t} + i\omega t - 1), \quad (3)$$

$$\gamma_k(\omega) = \frac{1}{\pi} |\text{Im} \Sigma_k(\omega + \varepsilon_k)|. \quad (4)$$

The kernel  $\gamma_k(\omega)$  (Fig. 1 top) from the imaginary part of  $\Sigma^{GW}(\omega)$  reflects the quasi-boson excitation spectrum in the system, with peaks corresponding to those in  $W(\omega) \propto \text{Im} \Sigma_k(\omega + \varepsilon_k)$ .

The basic ingredients in the theory Eq. (1-3), are thus  $G^0$ , the  $GW$  self-energy  $\Sigma^{GW}$ , and the screened Coulomb interaction  $W(q, \omega) = \epsilon^{-1}(q, \omega) v_q$ , where  $\epsilon(q, \omega)$  is the dielectric function. These quantities can be calculated using standard FT MBPT [1, 27], starting from the Matsubara Green's function. The FT analog of the  $GW$  self energy for electrons coupled to bosons is (cf. the Migdal approximation [1])

$$\Sigma^{GW}(\omega, T) = \int d\omega' \frac{d^3 q}{(2\pi)^3} |\text{Im} W(q, \omega')| \times \left[ \frac{f(\varepsilon_{k-q}) + N(\omega')}{\omega + \omega' - \varepsilon_{k-q} + i\delta} + \frac{1 - f(\varepsilon_{k-q}) + N(\omega')}{\omega - \omega' - \varepsilon_{k-q} + i\delta} \right]. \quad (5)$$

Here  $N(\omega) = 1/(e^{\beta\omega} - 1)$  is the Bose factor,  $f(\varepsilon) = 1/(e^{\beta(\varepsilon-\mu)} + 1)$  the Fermi factor,  $\beta = 1/k_B T$ , and  $\mu(T)$  is the chemical potential, as determined below. At high- $T$  the behavior of  $\gamma_k$  is dominated by the Bose factors  $N(\omega) \sim k_B T/\omega$  ( $T \rightarrow \infty$ ), and becomes strongly symmetric about  $\omega = 0$ . To obtain  $W$  we use for simplicity the FT-RPA approximation for the dielectric function

$$\epsilon(q, \omega) = 1 + 2v_q \int \frac{d^3k}{(2\pi)^3} \frac{f_{k+q} - f_k}{\omega - \varepsilon_{k+q} + \varepsilon_k}. \quad (6)$$

The imaginary part of  $\epsilon(q, \omega)$  is analytic [54, 55], and the real part is calculated via a Kramers-Kronig transform. This yields the FT loss function  $L(q, \omega) = |\text{Im} \epsilon^{-1}(q, \omega)|$ . For the HEG  $L(q > 0, \omega)$  exhibits broadened and blue-shifted plasmon-peaks with increasing  $T$  [55]. The chemical potential  $\mu = \mu(T, N)$  implicit in the Fermi factors  $f(\omega)$ , is determined by enforcing charge conservation  $\sum_{\mathbf{k}} n_{\mathbf{k}} = \langle N(T) \rangle$ , where the occupation numbers  $n_{\mathbf{k}}(T)$  are given by a trace over over  $A_{\mathbf{k}}(\omega)$  [44]

$$n_{\mathbf{k}}(\mu, T) = \int_{-\infty}^{\infty} d\omega A_{\mathbf{k}}(\omega) f(\omega). \quad (7)$$

Values of  $n_{\mathbf{k}}(T)$  can be measured by Compton scattering [56–58] and are sensitive to the many-body correlation effects in  $A_{\mathbf{k}}$ . At low- $T$ ,  $A_{\mathbf{k}}(\omega)$  exhibits multiple-satellites for  $k < k_F$ , while for  $k > k_F$  and at  $T > T_F$ , the quasi-particle peak broadens, and overlaps the satellites. Thus in WDM the structure of  $A_{\mathbf{k}}$  blurs into single asymmetric peak with a centroid at  $\varepsilon_k^x(T)$  and root mean square width  $\delta_k$  given by the 2nd cumulant moment of  $A_{\mathbf{k}}(\omega)$   $\delta_k^2 = \tilde{C}_k''(0) = \int d\omega \gamma_k(\omega)$ .

A dimensionless measure of correlation strength [32] is the satellite magnitude in the spectral function  $a_k \equiv \ln(1/Z_k) = \int d\omega \gamma_k(\omega)/\omega^2$ , where the renormalization constant  $Z_k$  is determined from the last term in Eq. (3). This measure characterizes corrections to the quasi-particle approximation and corresponds to the mean number of bosonic satellites. For plasmons in the HEG,  $a_k \approx 0.2r_s^{3/4} = 0.56$  at  $r_s = 4$  and  $T = 0$ , where  $r_s$  is the Wigner-Seitz radius; surprisingly  $a_k$  is only weakly dependent on temperature so that correlation effects remain strong at high  $T$ . Formally the structure of the cumulant in Eq. (3) is consistent with the conventional quasi-particle picture, i.e., a renormalized main peak red-shifted by a “relaxation energy”  $\Delta_k$  and a series of satellites. The correlation part of the quasi-particle energy shift  $\Delta_k$  is obtained from middle term in Eq. (3), while the first term gives rise to satellites at multiples of the plasmon peak  $\omega_p$ . The quasi-particle energy is then  $\varepsilon_k^{qp} = \varepsilon_k + \Delta_k$ , where

$$\Delta_k = \Sigma_k^x + \int d\omega \frac{\gamma_k(\omega)}{(\omega - i\delta)}. \quad (8)$$

The real part  $\Delta_k'$  is the relaxation energy which is comparable to that in QPSCGW [30]. Due to the increasingly

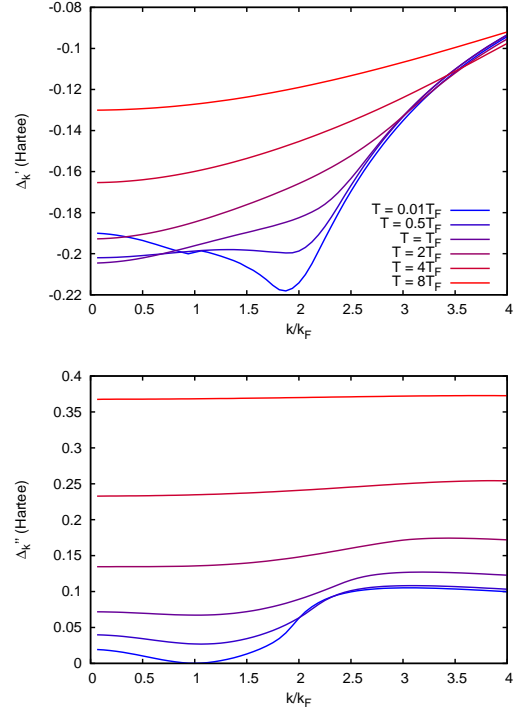


FIG. 2: (Color online) Real (top) and imaginary (bottom) parts of the quasiparticle energy correction  $\Delta_k$  for varying temperature.

symmetrical behavior of  $\gamma_k(\omega)$ ,  $\Delta_k'$  decreases smoothly with  $T$ . However, a striking difference with the  $T = 0$  behavior is the presence of an imaginary part  $\Delta_k''$  even at the Fermi momentum, which becomes large at high- $T$  since  $\gamma_k(0) \neq 0$ . This behavior implies strongly damped propagators that blur the usual quasi-particle picture, smearing band-gaps and band-structures. This broadening is clearly evident in the spectral function  $A_{\mathbf{k}}(\omega) = (1/\pi)|\text{Im} G_{\mathbf{k}}(\omega)|$  [27, 44] (Fig. 1), which is directly related to x-ray photoemission spectra (XPS). In contrast, the GW spectral function retains satellite structure even at high  $T$  (Fig. 1 inset).

One of the advantages of the cumulant formalism is that it provides an alternative for calculations of thermodynamic equilibrium properties. Remarkably, knowledge of  $\mu(T)$  is sufficient to determine the FT DFT exchange-correlation potential for the HEG [59] since  $v_{xc}(T) \equiv \mu_{xc}(T) = \mu(T) - \mu_0(T)$ , where  $\mu_0(T)$  is the chemical potential for non-interacting electrons (Fig. 3). Moreover, the FT total internal energy per particle  $\varepsilon(T) \equiv E(T)/N$ , can be calculated from the GMK sum-rule [27, 44, 45],

$$\varepsilon(T) = \sum_{\mathbf{k}} \int d\omega [\omega + \varepsilon_{\mathbf{k}}] A_{\mathbf{k}}(\omega) f(\omega) \equiv \varepsilon_H + \varepsilon_{xc}, \quad (9)$$

which is valid for any Hamiltonian with only pair interactions. This relation is similar in form to the zero- $T$  Galitskii-Migdal sum-rule, except for the Fermi fac-

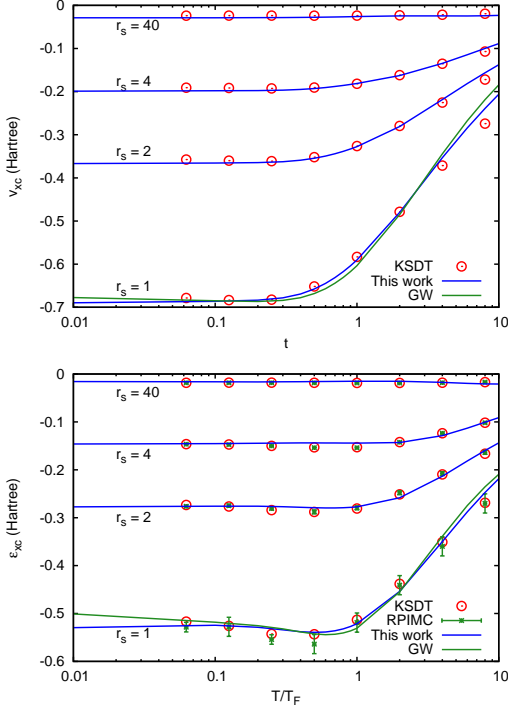


FIG. 3: (Color online) Finite- $T$  exchange-correlation potential  $v_{xc}$  (top) and exchange-correlation internal energy per particle  $\varepsilon_{xc}$  vs  $\tau = T/T_F$  (bottom) for the HEG from the cumulant expansion (blue), compared to PIMC[16] (crosses) and fits to FT-DFT[14] (red circles). Additional results are given in the Supplementary Material.

tor. The exchange-correlation internal energy  $\varepsilon_{xc}(T)$  is then obtained by subtracting the Hartree part  $\varepsilon_H$ , and results for the HEG are shown in Fig. 3. Clearly the agreement between the cumulant results, path-integral Monte Carlo (PIMC) calculations [16], and fits to FT-DFT functionals [14] is quite good. Calculations of the exchange-correlation free-energy require an additional entropic contribution [31]. At  $T = 0$ ,  $\varepsilon_{xc}$  was slightly better with the retarded cumulant than with  $G_0W_0$ , but self-consistent  $GW$  gave better total internal energies [33]. Finally, we calculate the Compton spectrum  $J_q(\omega)$  following Ref. [60],

$$J_q(\omega) = \int d^3k \, d\omega' \, A_{\mathbf{k}}(\omega') A_{\mathbf{k}+\mathbf{q}}(\omega + \omega') f(\omega') f(\omega + \omega'). \quad (10)$$

At small  $T$ , effects of correlation are quite noticeable (Fig. 4), leading to an effective temperature  $T^*$  (i.e. the temperature at which free-electron calculations match the interacting ones) of  $(T^* - T)/T_F \approx 0.3$  (see inset), while at high- $T$  the effect is smaller but non-negligible,  $(T^* - T)/T_F \approx 0.1$ . These results may be important in calibrating Compton scattering as a potential “thermometer” for WDM [56].

In summary we have developed a finite- $T$  Green’s function approach for calculations of excited state and ther-

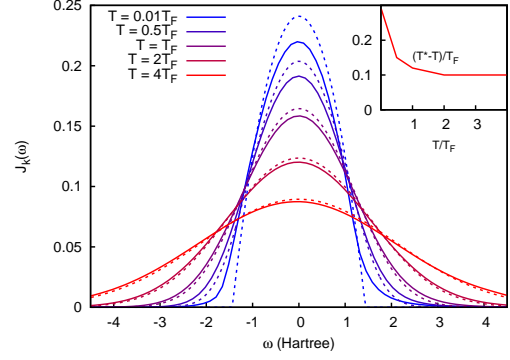


FIG. 4: (Color online) Finite- $T$  Compton spectrum compared to the free-electron  $T = 0$  result at  $r_s = 4$  and  $q = 3 \text{ Bohr}^{-1}$ . The inset shows the difference between the effective temperature  $T^*$  at which the free-electron calculation matches the cumulant result at  $T$ .

modynamic properties over a wide range of densities and temperatures. Our approach is based on the retarded cumulant expansion to first order in  $W$ . This approximation greatly simplifies the theory and provides a practical approach both for calculations and the interpretation of exchange and correlation effects in terms of the retarded cumulant  $C_k(t)$  or equivalently, the FT  $GW$  self energy  $\Sigma^{GW}$ . Thus the method provides an attractive alternative to FT DFT and QMC methods, which are not directly applicable to many excited state properties and spectra. The cumulant GF builds in an approximate dynamic vertex, going beyond the  $GW$  approximation, yet is no more difficult to calculate. Illustrative results for the HEG explain the crossover in behavior from cool to WDM regimes and the blurring of the conventional quasi-particle picture. Although the calculations here are for the spin-unpolarized case, the generalization to polarized calculations is in progress. Also, although we have focused on the HEG, reflecting the importance of density fluctuations at high- $T$ , the cumulant can be generalized to include other quasi-boson excitations such as phonons since the leading cumulant is linear in bosonic couplings [46]. We find that correlation corrections remain strong even at high  $T$ . Calculations of thermodynamic equilibrium quantities including exchange-correlation internal energies and potentials are in good agreement - typically within a few percent - with existing quantum PIMC calculations. Many extensions are possible, ranging from excited state and spectra to the thermodynamic properties of realistic systems, and potentially to the development of improved FT DFT functionals [9].

**Acknowledgments:** We thank K. Burke, G. Bertsch, V. Karasiev, L. Reining, E. Shirley, G. Seidler, T. Devereaux, and S. Trickey for comments and suggestions. This work is supported by DOE BES Grant DE-FG02-97ER45623.

- 
- [1] P. B. Allen and B. Mitrović, in *Solid State Physics*, edited by H. Ehrenreich, F. Seitz, and D. Turnbull (Academic Press, 1982), vol. 37, pp. 1–92.
- [2] P. Allen and V. Heine, *J. Phys. C* **9**, 2305 (1976).
- [3] A. Eiguren and C. Ambrosch-Draxl, *Phys. Rev. Lett.* **101**, 036402 (2008).
- [4] M. Koenig, A. Benuzzi-Mounaix, A. Ravasio, T. Vinci, N. Ozaki, S. Lepape, D. Batani, G. Huser, T. Hall, D. Hicks, et al., *Plasma Phys. Control. Fusion* **47**, B441 (2005).
- [5] S. Glenzer, H. Lee, P. Davis, T. Dppner, R. Falcone, C. Fortmann, B. Hammel, A. Kritcher, O. Landen, R. Lee, et al., *High Energy Density Physics* **6**, 1 (2010).
- [6] K. P. Driver and B. Militzer, *Phys. Rev. B* **93**, 064101 (2016).
- [7] M. W. C. Dharma-wardana, *J. Phys.: Conf. Ser.* **442**, 012030 (2013).
- [8] T. Sjostrom and J. Dufty, *Phys. Rev. B* **88**, 115123 (2013).
- [9] K. Burke, J. C. Smith, P. E. Grabowski, and A. Pribram-Jones, *Phys. Rev. B* **93**, 195132 (2016).
- [10] A. Pribram-Jones and K. Burke, *Phys. Rev. B* **93**, 205140 (2016).
- [11] P. Hohenberg and W. Kohn, *Phys. Rev.* **136**, B864 (1964).
- [12] W. Kohn and L. J. Sham, *Phys. Rev.* **140**, A1133 (1965).
- [13] N. D. Mermin, *Phys. Rev.* **137**, A1441 (1965).
- [14] V. V. Karasiev, T. Sjostrom, J. Dufty, and S. B. Trickey, *Phys. Rev. Lett.* **112**, 076403 (2014), see especially supplementary materials.
- [15] V. V. Karasiev, L. Calderín, and S. B. Trickey, *Phys. Rev. E* **93**, 063207 (2016).
- [16] E. W. Brown, B. K. Clark, J. L. DuBois, and D. M. Ceperley, *Phys. Rev. Lett.* **110**, 146405 (2013).
- [17] G. G. Spink, R. J. Needs, and N. D. Drummond, *Phys. Rev. B* **88**, 085121 (2013).
- [18] S. Tanaka and S. Ichimaru, *J. Phys. Soc. Jpn.* **55**, 2278 (1986).
- [19] K. S. Singwi, M. P. Tosi, R. H. Land, and A. Sjölander, *Phys. Rev.* **176**, 589 (1968).
- [20] Z. Yan, J. P. Perdew, and S. Kurth, *Phys. Rev. B* **61**, 16430 (2000).
- [21] T. Dornheim, S. Groth, T. Sjostrom, F. D. Malone, W. M. C. Foulkes, and M. Bonitz, *Phys. Rev. Lett.* **117**, 156403 (2016).
- [22] G. Onida, L. Reining, and A. Rubio, *Rev. Mod. Phys.* **74**, 601 (2002).
- [23] R. M. Martin, L. Reining, and D. M. Ceperley, *Interacting Electrons, Theory and Computational Approaches* (Cambridge University Press, Cambridge, 2016).
- [24] A. Zangwill and P. Soven, *Phys. Rev. A* **21**, 1561 (1980).
- [25] B. I. Cho, K. Engelhorn, A. A. Correa, T. Ogitsu, C. P. Weber, H. J. Lee, J. Feng, P. A. Ni, Y. Ping, A. J. Nelson, et al., *Phys. Rev. Lett.* **106**, 167601 (2011).
- [26] A. Pribram-Jones, P. E. Grabowski, and K. Burke, *Phys. Rev. Lett.* **116**, 233001 (2016).
- [27] G. Mahan, *Many-Particle Physics* (Springer, 2000).
- [28] S. Engelsberg and J. R. Schrieffer, *Phys. Rev.* **131**, 993 (1963).
- [29] A. Rios, A. Polls, A. Ramos, and H. Mütter, *Phys. Rev. C* **78**, 044314 (2008).
- [30] S. V. Faleev, M. van Schilfgaarde, T. Kotani, F. Léonard, and M. P. Desjarlais, *Phys. Rev. B* **74**, 033101 (2006).
- [31] M. Dharma-wardana and R. Taylor, *J. Phys. C: Solid State Phys.* **14**, 629 (1981).
- [32] L. Hedin, *J. Phys.: Condens. Matter* **11**, R489 (1999).
- [33] J. J. Kas, J. J. Rehr, and L. Reining, *Phys. Rev. B* **90**, 085112 (2014).
- [34] J. Zhou, J. Kas, L. Sponza, I. Reshetnyak, M. Guzzo, C. Giorgetti, M. Gatti, F. Sottile, J. Rehr, and L. Reining, *J. Chem. Phys.* **143** (2015).
- [35] D. C. Langreth, *Phys. Rev. B* **1**, 471 (1970).
- [36] M. Guzzo, G. Lani, F. Sottile, P. Romaniello, M. Gatti, J. J. Kas, J. J. Rehr, M. G. Silly, F. Sirotti, and L. Reining, *Phys. Rev. Lett.* **107**, 166401 (2011).
- [37] F. Aryasetiawan, L. Hedin, and K. Karlsson, *Phys. Rev. Lett.* **77**, 2268 (1996).
- [38] J. J. Kas, F. D. Vila, J. J. Rehr, and S. A. Chambers, *Phys. Rev. B* **91**, 121112(R) (2015).
- [39] A. J. Lee, F. D. Vila, and J. J. Rehr, *Phys. Rev. B* **86**, 115107 (2012).
- [40] J. J. Kas, J. J. Rehr, and J. B. Curtis, *Phys. Rev. B* **94**, 035156 (2016).
- [41] J. Lischner, D. Vigil-Fowler, and S. G. Louie, *Phys. Rev. B* **89**, 125430 (2014).
- [42] F. Caruso, H. Lambert, and F. Giustino, *Phys. Rev. Lett.* **114**, 146404 (2015).
- [43] F. Caruso and F. Giustino, *Phys. Rev. B* **92**, 045123 (2015).
- [44] P. C. Martin and J. Schwinger, *Phys. Rev.* **115**, 1342 (1959).
- [45] D. S. Koltun, *Phys. Rev. C* **9**, 484 (1974).
- [46] S. M. Story, J. J. Kas, F. D. Vila, M. J. Verstraete, and J. J. Rehr, *Phys. Rev. B* **90**, 195135 (2014).
- [47] L. Dash, H. Ness, and R. Godby, *J. Chem. Phys.* **132**, 104113 (2010).
- [48] M. S. Hybertsen and S. G. Louie, *Phys. Rev. Lett.* **55**, 1418 (1985).
- [49] O. Gunnarsson, V. Meden, and K. Schönhammer, *Phys. Rev. B* **50**, 10462 (1994).
- [50] Y. Pavlyukh, J. Berakdar, and A. Rubio, *Phys. Rev. B* **87**, 125101 (2013).
- [51] X. Deng, J. Mravlje, R. Žitko, M. Ferrero, G. Kotliar, and A. Georges, *Phys. Rev. Lett.* **110**, 086401 (2013).
- [52] M. Casula, A. Rubtsov, and S. Biermann, *Phys. Rev. B* **85**, 035115 (2012).
- [53] L. Landau, *J. Phys. USSR* **8**, 201 (1944).
- [54] F. C. Khanna and H. R. Glyde, *Can. J. Phys.* **54**, 648 (1976).
- [55] N. R. Arista and W. Brandt, *Phys. Rev. A* **29**, 1471 (1984).
- [56] B. A. Mattern, G. T. Seidler, J. J. Kas, J. I. Pacold, and J. J. Rehr, *Phys. Rev. B* **85**, 115135 (2012).
- [57] E. Klevak, J. J. Kas, and J. J. Rehr, *Phys. Rev. B* **89**, 085123 (2014).
- [58] S. Huotari, J. A. Soininen, T. Pylkkänen, K. Hämäläinen, A. Issolah, A. Titov, J. McMinis, J. Kim, K. Esler, D. M. Ceperley, et al., *Phys. Rev. Lett.* **105**, 086403 (2010).
- [59] F. Perrot, , and M. W. C. Dharma-wardana, *Phys. Rev. B* **62**, 16536 (2000).
- [60] W. Schülke, G. Stutz, F. Wohler, and A. Kaprolat, *Phys. Rev. B* **54**, 14381 (1996).